JOURNAL OF THERMOPHYSICS AND HEAT TRANSFER
Vol. 24, No. 1, January–March 2010

Theoretical Studies of Hard Filling in Loop Heat Pipes

Abhijit A. Adoni,* Amrit Ambirajan,† V. S. Jasvanth,† and D. Kumar†
Indian Space Research Organisation, Bangalore 560 017, India
and
Pradip Dutta‡
Indian Institute of Science, Bangalore 560 012, India

DOI: 10.2514/1.44382

Loop heat pipe is a passive two-phase heat transport device that is gaining importance as a part of spacecraft thermal control systems and also in applications (such as in avionic cooling and submarines). Hard fill of a loop heat pipe occurs when the compensation chamber is full of liquid. A theoretical study is undertaken to investigate the issues underlying the loop heat pipe hard-fill phenomenon. The results of the study suggest that the mass of charge and the presence of a bayonet have significant impact on the loop heat pipe operation. With a larger mass of charge, a loop heat pipe hard fills at a lower heat load. As the heat load increases, there is a steep rise in the loop heat pipe operating temperature. In a loop heat pipe with a saturated compensation chamber, and also in a hard-filled loop heat pipe without a bayonet, the temperature of the compensation chamber and that of the liquid core are nearly equal. When a loop heat pipe with a bayonet hard fills, the compensation chamber and the evaporator core temperatures are different.

Nomenclature

A	=	area (general flow area), m^2
C_p	=	specific heat at constant pressure, $J \cdot kg^{-1} \cdot K^{-1}$
D	=	diameter, m
H	=	heat transfer coefficient, $W \cdot m^{-2} \cdot K^{-1}$
K	=	wick permeability, m^2
k	=	thermal conductivity, $W \cdot m^{-1} \cdot K^{-1}$
L	=	length, m
M	=	mass of working fluid, kg
$\dot{m}$	=	mass flow rate, $kg \cdot s^{-1}$
P	=	pressure, Pa
Q	=	rate of heat transfer, W
r	=	radius, m
T	=	temperature, K
t	=	thickness, m
U	=	overall heat transfer coefficient, $W \cdot m^{-2} \cdot K^{-1}$
x	=	vapor quality
z	=	length, m
β	=	volume fraction of liquid in the compensation chamber
Γ	=	perimeter, m
λ	=	conductance, $W \cdot K^{-1}$
ϵ	=	porosity
ρ	=	density, $kg \cdot m^{-3}$

Subscripts

b	=	bayonet
c	=	core
cond	=	condenser
cond′	=	two-phase region in the condenser
evap	=	evaporator
fg	=	difference in the thermodynamic property in the liquid and vapor phase
hf	=	loop heat pipe is hard-filled
i	=	inner part of tube
L	=	heat leak
l	=	liquid
ll	=	liquid line
load	=	heat load applied externally
o	=	outer part of the tube
open	=	condenser is open
r	=	compensation chamber
sink	=	sink of the condenser
t	=	tube/evaporator teeth
tot	=	total
v	=	vapor
vl	=	vapor line
w	=	wick
z	=	length direction
0	=	just above the meniscus
1	=	exit of the evaporator
2	=	exit of the vapor line/entry of the condenser
2cond	=	saturated liquid (point at which condensation is finished in the condenser)
2scv	=	saturated vapor (end of the sensible cooling of vapor in the condenser)
3	=	exit of the condenser/entry to the liquid line
4	=	exit of the liquid line and entry to the bayonet
4e	=	fluid in the bayonet at the border of the compensation chamber and the core
5	=	evaporator core
∞	=	ambient/surrounding

Received 16 March 2009; revision received 30 July 2009; accepted for publication 30 July 2009.

*Engineer, Satellite Centre, Thermal Systems Group; abhijit@isac.gov.in.
†Engineer, Satellite Centre, Thermal Systems Group.
‡Professor, Department of Mechanical Engineering.

I. Introduction

LOOP heat pipes (LHP) are increasingly being used for the thermal management of high heat dissipating electronic devices. The operating principle of an LHP is similar to that of a conventional heat pipe; however, the former has a higher heat transport capacity. Figure 1 shows a schematic of an LHP. Smooth tubes (liquid and vapor) connect the capillary evaporator to the condenser. In contrast to the distributed capillary structure of a heat pipe, the capillary structure in an LHP is limited to the evaporator. This results in a considerably lower pressure drop within the wick of an LHP. A two-phase reservoir called the compensation chamber (CC) is located adjacent to the evaporator. It exchanges liquid with the rest of the loop, depending on the heat load. A detailed

description of the working principle of LHPs and the closely related capillary pumped loops (CPLs) can be found in [1–3].

A tubular axially grooved (TAG) evaporator of an LHP is often equipped with a bayonet to route the liquid in the core (of the evaporator). In an LHP typically designed for terrestrial applications, the liquid returning from the condenser directly enters the CC [2,4]. However, a bayonet is used in LHPs for applications in microgravity [4]. A secondary wick is often used to ensure that the primary wick is always saturated with liquid and also to provide a good thermal link between the CC and the core.

An LHP is termed hard-filled when the CC is full of (subcooled) liquid. The heat load at which it hard fills depends on the mass of working fluid in the loop. The variation of the operating temperature with the heat load is approximately linear in a hard-filled LHP [2,3]. Linear behavior also occurs in a non-hard-filled LHP when the condenser is fully used. An LHP with a saturated CC (non-hard-filled) has a good thermal and hydraulic coupling with the core. In essence, it is almost an extension of the core.

Ku [1,5] and Maidanik [2] gave a brief chronology of developments in CPLs and LHPs and reviewed advances in CPL/LHP technology. Kaya and Hoang [6] presented a mathematical model for steady-state thermohydraulic performance of an LHP. Chuang [7] extended the preceding model to analyze the effect of adverse tilt on steady-state performance and experimentally validated the same. Recently, Launay et al. [8] presented an analytical approach to modeling of an LHP operating in the conventional mode (i.e., an LHP with a two-phase CC). They derived separate expressions for the operating temperature in the variable conductance and constant conductance modes. In an LHP, constant conductance mode occurs if the CC is hard-filled [2] or if the condenser fully opens [5]. Adoni et al. [3] presented a model that assumed that the thermodynamic state of the CC and the core were identical. No assumption was made about the state of the core, thus enabling the model to handle extreme conditions such as hard fill. This model assumed that the temperature of the CC and the core were identical, which was applicable to LHPs without a bayonet.

The preceding theoretical and experimental studies have significantly improved the steady-state mathematical modeling of the LHP with a two-phase CC and, to some extent, the hard-filled LHP. However, the authors are yet to come across mathematical models that deal with the effect of the bayonet on operational characteristics of an LHP with a hard-filled CC. Although LHP systems are not generally designed for hard filling under normal operating conditions, knowledge of their performance with a hard-filled CC would be useful in deciding about design margins. Further, recent literature [2,9] shows that hard-filled LHP designs are gaining prominence. In LHPs with multiple evaporators, all the CCs are hard-filled except the one that is controlling the operating temperature of the loop [5]. In this paper, aspects of steady-state thermohydraulic modeling are presented to study the hard-fill effects and the presence of a bayonet on the operating characteristics of an LHP with a TAG evaporator.

II. Loop Heat Pipe Mathematical Model

The goal of the LHP mathematical model is to determine the operating temperatures and pressures at various locations in the loop as a function of input power. The input parameters for the steady-state model of the LHP are sink temperature, ambient temperature, mass of charge (working fluid), physical dimensions of various components, and thermophysical properties of the working fluid. This section outlines the mathematical formulation for evaluating the temperatures and pressures at the state points (0, 1, 2, 2scv, 2cond, 3, 4, 4e, 5, and r) shown in Fig. 1. The heat exchange and the pressure drop in the wick, the vapor line, the liquid line, and the condenser of an LHP have been elaborately discussed in [3,6,10]. In this paper, the authors primarily focus on the mathematical modeling of heat exchange between the core, the CC, and the bayonet (in a TAG evaporator) of an LHP. The energy equations developed in this section will be used to estimate the thermodynamic state of the core and the CC. These equations, in conjunction with the energy and momentum equations for other components in the loop, are solved using algorithms presented in [3,10].

In an LHP, the CC is thermally and hydraulically connected to the core of the evaporator. For LHPs with flat plate (FP) evaporators, the CC is the core. The CC in an LHP with a TAG evaporator is generally located at one end of the evaporator. A bayonet is often provided to route the fluid entering the evaporator to the core (in a TAG evaporator) and through the CC (Fig. 1). In a TAG evaporator, the secondary wick is used to thermally and hydraulically connect the CC and the core. The secondary wick at all times keeps the primary wick wetted (especially in microgravity condition). It also helps isothermalize the core and the CC by a mechanism analogous to that of heat pipes. This is only possible if the fluid in the CC and the core is saturated (two phase). In a hard-filled LHP with a TAG evaporator, the isothermalization mechanism attributed to the secondary wick ceases to exist because vapor is not present. Thus, in an LHP, the saturated (two-phase) CC and the hard-filled CC must be modeled in different ways:

1) For the two-phase CC, the saturated CC/core is solved using methodology identical to that described in [3,10]. The thermodynamic state of the CC and the core is identical due to good thermal/fluid coupling between them. The bayonet does not influence the steady-state performance with a two-phase CC. In this case, the combined energy balance of the CC and the core [Eq. (3)] is used to obtain the operating temperature T_0.

2) For the hard-filled CC, in general, the core and the CC can have different temperatures. The presence of a bayonet significantly

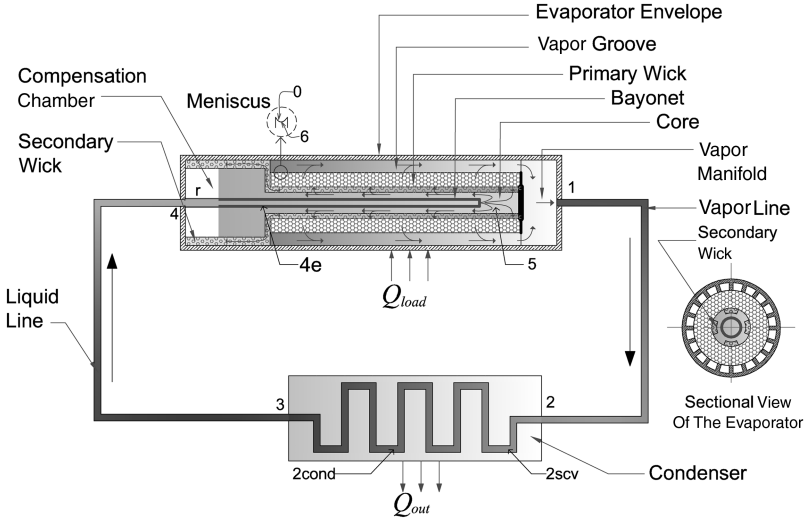

Fig. 1 Schematic of an LHP with a TAG evaporator.

influences the thermodynamic state of the core and the CC, which in turn influences the steady-state operating temperature of the loop. The formulations in Secs. II.B–II.D result in equations that are solved for T_{4e}, ρ_{4e}, T_5, ρ_5, T_r, and ρ_r (the thermodynamic state of the core and the CC) with given T_0, $\dot{m}$, x_4, P_4, and T_4. These three sections consider the following cases:

a) $T_r = T_5$ [i.e., the core and the CC are assumed to be identical (typically FP evaporator)].

b) No bayonet is present (i.e., the liquid line terminates in the CC of a TAG evaporator).

c) $T_r \neq T_5$, where the bayonet is present and it delivers the liquid from the liquid line directly to the core of the evaporator.

In this section, the methodology for determining the thermodynamic state of the core and the CC under various modes of operation is presented. The following sections delineate the formulation of heat transfer in the CC and the core under various modes of operation and also for various configurations. The model presented here does not account for gravity effects on LHP operating characteristics.

A. Saturated Compensation Chamber

In this analysis of LHPs, the core (state point 5 in Fig. 1) and the CC (state point r) are assumed to be isothermal and saturated until hard fill occurs. Thus, the thermodynamic states of the CC and the core are identical. In an LHP with a two-phase saturated CC (with or without a bayonet),

$$P_5(T_5,\ \rho_5) = P_4 \tag{1}$$

$$T_5 = T_{\text{sat}}(P_5) \tag{2}$$

$T_{\text{sat}}(P_5)$ is the saturation temperature corresponding to pressure P_5. Equation (1) assumes that the pressure drop in the bayonet (if present) is negligible and the pressure in the CC/core is nearly equal to that at the liquid line exit. Note that the equation of state $[P_5(T_5,\ \rho_5)$ and $T_{\text{sat}}(P_5)]$ in Eqs. (1) and (2) is obtained from REFPROP 7.0 [11]. The energy balance equation for the LHP core and the CC (together) is

$$Q_{Lc} + Q_{\text{evap}-r} + x_4\dot{m}h_{\text{fg},5} = \underbrace{A_r U_{r-\infty}(T_r - T_\infty)}_{\text{loss to ambient}} + \underbrace{\dot{m}C_{p,54}(T_5 - T_4)}_{\text{sensible cooling}} \tag{3}$$

Q_{Lc} and $Q_{\text{evap}-r}$ are evaluated based on a procedure outlined in [3,10]. Heat leak to the core of the wick Q_{Lc} is a function of T_0, T_5, wick properties, working fluid properties, and mass flow rate $\dot{m}$. For a TAG evaporator [3],

$$Q_{Lc} = \frac{\dot{m}C_{p,05}(D_{wi}/D_{wo})^{(\dot{m}C_{p,05}/2\pi k_{we}L_w)}(T_0 - T_5)}{1 - (D_{wi}/D_{wo})^{(\dot{m}C_{p,05}/2\pi k_{we}L_w)}} \tag{4}$$

where $C_{p,05}$ is the mean working fluid specific heat between 0 and 5. The expression for heat leak from the evaporator casing to the CC $Q_{\text{evap}-r}$ is given by

$$Q_{\text{evap}-r} = \lambda_{\text{evap}-r}(T_{\text{evap}} - T_r) \tag{5}$$

The third term on the left-hand side of Eq. (3) is the latent heat that is rejected when the fluid entering the core contains vapor (i.e., $x_4 > 0$). The first term on the right-hand side of Eq. (3) accounts for the heat exchange between the CC and the ambient $Q_{r-\infty}$, and the second term represents the sensible cooling due to the liquid entering the core. Equation (3) is solved iteratively for T_0. As the core and the CC are assumed to have identical thermodynamic states, T_r is equal to T_5.

The method outlined here is identical to previous theoretical treatments [3,6] for an LHP operating with a two-phase CC. The algorithm called A1-LHP, as described in [3], can be used for numerical evaluation of the various state points.

B. Hard-Filled Loop Heat Pipe: Assuming T_r–T_5

For a hard-filled LHP with good thermal and fluidic coupling between the CC and the core, the thermodynamic state of the core and the CC are assumed to be the same. This occurs in an LHP with an FP evaporator for which the core and the CC are the same. It may also occur in a TAG LHP that does not have a bayonet, wherein the fluid first enters the CC before reaching the core. In this case, the CC and the core temperatures are nearly the same (Sec. IV.B). However, the two temperatures may be significantly different when a TAG LHP with a bayonet hard fills (Sec. IV.C).

The solution methodology is identical to the previous theoretical treatment [3] of an LHP operating with a hard-filled CC. The algorithm called A2, as described in [3], can be used for numerical evaluation of various state points in such an LHP. In Algorithm A2, the thermodynamic state of the core and the CC is obtained by simultaneously solving the equation of state (1) and the energy balance equation in the core [Eq. (3)] for T_5 and ρ_5. The mass balance equation, as described in [3], is used to determine the thermodynamic state just above the meniscus (state point 0).

C. Hard-Filled Tubular Axially Grooved Loop Heat Pipes Without a Bayonet

This section presents a methodology to estimate the thermodynamic state of the core and the CC in an LHP without a bayonet. The fluid leaving the liquid line directly enters the CC and then the core. The solution methodology outlined in this section does not assume that the temperatures of the CC and the core are identical.

The equation of state (6) and the energy balance equation (7) for the CC are, respectively,

$$P_r(T_r,\ \rho_r) = P_4 \tag{6}$$

$$\underbrace{U_{r-\infty}A_r(T_r - T_\infty)}_{Q_{r-\infty}} = \underbrace{\lambda_{c-r}(T_5 - T_r)}_{Q_{c-r}} + \underbrace{\lambda_{\text{evap}-r}(T_{\text{evap}} - T_r)}_{Q_{\text{evap}-r}} + \dot{m}C_{p,4r}(T_4 - T_r) + \dot{m}x_4h_{\text{fg}} \tag{7}$$

$C_{p,4r}$ is the average of the specific heat evaluated at state points 4 and r. Note that the equation of state $[P_r(T_r,\ \rho_r)]$ in Eq. (6) is obtained from REFPROP 7.0 [11]. The energy balance in the core is given by

$$\underbrace{\lambda_{c-r}(T_5 - T_r)}_{Q_{c-r}} = Q_{\text{Lc}} + \dot{m}C_{p,5r}(T_r - T_5) \tag{8}$$

Equations (1) and (6–8) are solved simultaneously to obtain T_5, ρ_5, T_r, and ρ_r. The effective conductance between the core and the CC, λ_{c-r}, is obtained assuming a conductive thermal coupling through the liquid column in the CC tube.

It will be demonstrated later in this paper that, for a hard-filled LHP without a bayonet, the core and the CC temperatures are nearly equal to each other.

D. Hard-Filled Tubular Axially Grooved Loop Heat Pipes with a Bayonet

This section discusses the treatment of heat transfer and fluid flow in the CC and the core of a hard-filled LHP with a bayonet. The assumption that T_r is nearly equal to T_5 does not hold for a hard-filled LHP with a bayonet (Fig. 2b). There will be heat exchange between the CC and the core due to (significant) temperature difference. Heat exchange between them is assumed to occur by conduction through the intermediate liquid and the interconnecting tube wall. Under such conditions, if some vapor is present in the fluid leaving the liquid line, the vapor entering the core will migrate to the CC and condense. A corresponding mass of liquid will move to the core from the CC. Heat is also exchanged (Q_{b-r}) between the fluid in the bayonet (as it traverses the CC) and the fluid in the CC. Thus, the energy balance in the *CC* is given by

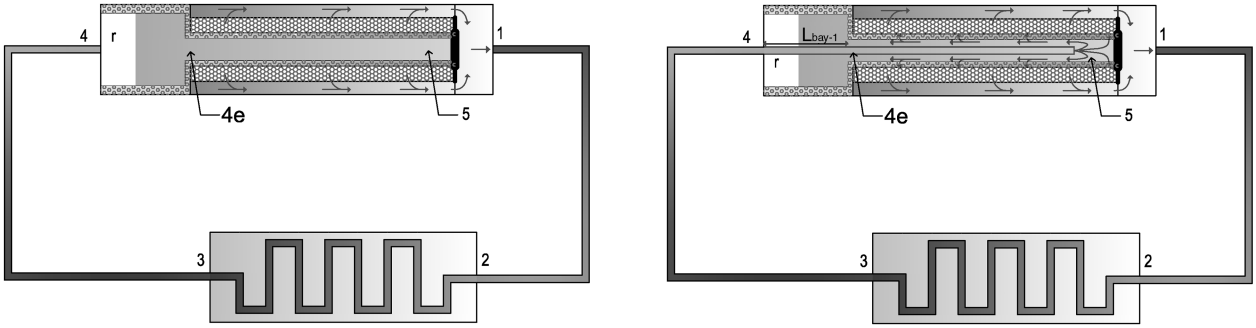

Fig. 2 Schematic showing an LHP a) without a bayonet and b) with a bayonet.

$$Q_{r-\infty} = Q_{b-r} + Q_{c-r} + Q_{\text{evap}-r} + \underbrace{\dot{m}x_{4e}h_{\text{fg}}}_{\text{enthalpy of condensation}} + \underbrace{x_{4e}\dot{m}C_{p,r4e}(T_{4e} - T_r)}_{\text{condensate sensible cooling}} \tag{9}$$

The evaluation of Q_{b-r} in Eq. (9) depends on whether hard fill occurs before or after the condenser fully opens. This is discussed later in Secs. II.D.1 and II.D.2. Q_{c-r} is the heat transfer by conduction from the core to the CC (reservoir) and is given by

$$Q_{c-r} = \lambda_{c-r}(T_5 - T_r) \tag{10}$$

$Q_{\text{evap}-r}$ is obtained using Eq. (5). The last two terms on the right-hand side of Eq. (9) arise from the assumption that all vapor entering the core of the evaporator migrates to the CC without undergoing any heat and mass exchange in the core. In spite of the vapor entering the core, an LHP does not deprime. The latent heat associated with the vapor leaving the liquid line is lost to the ambient in the CC [5,12]. The vapor condenses in the CC, and mass is conserved by reverse flow of liquid to the core. This implies that the operating temperature is higher than the ambient. The fourth term on the right-hand side of Eq. (9) is the enthalpy of condensation of the bubbles moving into the CC, and the last term represents sensible cooling of this condensed liquid in the CC. $C_{p,r4e}$ is the average specific heat between the state points r and $4e$. The secondary wick ensures this fluid exchange. The energy balance in the core is given by

$$Q_{c-r} + x_{4e}\dot{m}C_p(T_5 - T_r) = Q_{\text{Lc}} + (1 - x_{4e})\dot{m}C_{p54}(T_{4e} - T_5) \tag{11}$$

The second term on the right-hand side of Eq. (11) is the enthalpy gain associated with the liquid entering the core from the bayonet. Similarly, the second term on the left-hand side of the preceding equation is the enthalpy loss due to liquid flowing back to the core from the CC (subsequent to condensation). The pressures in the core, the CC, and at the exit of the liquid line are assumed to be the same [Eqs. (1) and (6)]. For a hard-filled LHP with a bayonet, the state of the core is obtained by simultaneously solving Eqs. (1), (9), and (11).

The energy equation for heat exchange between the bayonet and the CC fluid is

$$\dot{m}C_p\frac{\mathrm{d}T}{\mathrm{d}z} = -U_{b-r}\Gamma_b(T - T_r) \tag{12}$$

where C_p is evaluated at state point 4. The solution of the preceding ordinary differential equation (ODE) yields

$$T_4 - T_{4e} = (T_4 - T_r)\left[1 - \exp\left(\frac{-U_{b-r}A_b}{\dot{m}C_p}\right)\right] \tag{13}$$

where $4e$ is the point on the bayonet beyond which convective heat exchange between the fluid in the CC and the bayonet ceases (Fig. 2b). U_{b-r} is the overall heat transfer coefficient between the bayonet (fluid) and the CC (fluid), based on the inner diameter of the bayonet. In Eq. (13), A_{b-r} is the area of the bayonet (referenced to the bayonet inner surface) that is in contact with the fluid in the CC.

1. Hard Fill Occurring Before Complete Opening of the Condenser

If hard fill occurs before the condenser fully opens, heat exchange between the CC and the bayonet ($x_4 = 0$) is

$$Q_{b-r} = \dot{m}C_p(T_4 - T_{4e}) = \lambda_{b-r}(T_4 - T_r) \tag{14}$$

In the preceding equation, C_p is evaluated at state point 4, and λ_{b-r} is given by

$$\lambda_{b-r} = \dot{m}C_p\left[1 - \exp\left(\frac{-U_{b-r}A_{b-r}}{\dot{m}C_p}\right)\right]$$

2. Hard Fill Occurring After Complete Opening of the Condenser

When the condenser fully opens, any vapor present in the fluid entering the evaporator is condensed in the CC. If hard fill occurs after the condenser is fully open and some vapor is present in the fluid leaving the liquid line, the heat exchange in the bayonet is given by

$$Q_{b-r} = \lambda_{b-r}(T_4 - T_r) \tag{15}$$

If the vapor entering the bayonet from the liquid line is completely condensed in the region traversing the CC, λ_{b-r} is given by

$$\lambda_{b-r} \equiv U_{b-r-2ph}A_{b1-r} + \dot{m}C_p\left[1 - \exp\left(\frac{-U_{b-r-1ph}A_{b2-r}}{\dot{m}C_p}\right)\right]$$

A_{b1-r} is the heat exchange area in the two-phase region of the bayonet and A_{b2-r} is the area of the remaining (single-phase) length of the bayonet in contact with the fluid in the CC. They satisfy the relation $A_{b-r} = A_{b1-r} + A_{b2-r}$. $U_{b-r-2\text{ph}}$ and $U_{b-r-1\text{ph}}$ are overall heat transfer coefficients between the fluid in the bayonet and the fluid in the CC in regions associated with areas A_{b1-r} and A_{b2-r}, respectively. U_{b-r} ($U_{b-r-2\text{ph}}$ or $U_{b-r-1\text{ph}}$) is evaluated by

$$\frac{1}{U_{b-r}} = \frac{1}{H_{bi}} + \frac{D_{b,i}}{D_{b,o}H_{bo}} + \frac{D_{b,i}}{2k_{b,t}}\ln\left(\frac{D_{b,o}}{D_{b,i}}\right) \tag{16}$$

where H_{bo} is the heat transfer coefficient between the bayonet tube and surrounding fluid in the CC. This can vary from 25 to 100 $\text{W}/(\text{m}^2 \cdot \text{K})$, depending on the working fluid, and it is determined by a methodology outlined in [13]. For typical CC dimensions and using standard correlations, H_{bo} is approximated to be about 50 $\text{W}/(\text{m}^2 \cdot \text{K})$ in the analysis, presented in Sec. IV. If fluid in the bayonet is single phase, then H_{bi} is obtained from the Dittus–Boelter correlation [13] for turbulent flow in the bayonet or from the relation $Nu = 48/11$ for laminar flow. If $x_4 > 0$, then H_{bi} will be very large and its influence on U_{b-r} can be neglected, as the controlling thermal resistance in this case is attributed to H_{bo}. The heat transfer area A_{b1-r} is obtained from

$$A_{b1-r} = \left| \frac{\dot{m} h_{\mathrm{fg}} x_4}{U_{b-r-2ph}(T_4 - T_r)} \right| \tag{17}$$

If A_{b1-r} is greater than A_{b-r}, then the fluid does not completely condense in the bayonet L_{b1}, hence $A_{b1-r} = A_{b-r}$. The quality x_{4e} is calculated by

$$x_{4e} = x_4 - \left| \frac{U_{b-r-2\mathrm{ph}}(T_4 - T_r)}{\dot{m} h_{\mathrm{fg}}} \right| \tag{18}$$

III. Numerical Scheme

The numerical scheme adopted here is a variant of the fixed-point iteration technique [3,14] for a nonlinear system of equations and is used to predict temperature, pressure, and mass distribution in the loop. The Newton–Raphson method is also used to minimize energy balance residue and mass imbalance. There are ODEs to be solved for some components (viz., the vapor line, the liquid line, and the condenser [3,10]). Upon solving the ODEs, the thermodynamic state at the exit of the component is obtained. The fixed-point iteration scheme adopted here involves sequential solving of these equations, namely, ODEs or nonlinear equations, as discussed in [3,10].

The formulation presented in Sec. II is essentially equations for the core and the CC. As mentioned previously, these must be solved in conjunction with equations for the rest of the loop. Equations for the rest of the loop (i.e., the vapor line, the liquid line, and the condenser) are given in [3].

Table 1 summarizes the usage of various algorithms for the cases considered in this paper. [3] is used to determine various thermodynamic states in the loop for conditions described in Sec. II.A. Algorithm A2 [3] describes the methodology to determine the state points for conditions described in Sec. II.B. Algorithm A1-LHP calls Algorithm A0, which solves for all loop state points (using the loop and evaporator equations), given Q_{load}, T_{sink}, T_0, T_5, and T_∞. A1-LHP basically consists of an update equation for T_0 and repeatedly calls A0 until convergence is reached (global energy balance and T_0). Algorithm A2 is for hard-filled LHPs with $T_r \sim T_5$. It also repeatedly updates T_0 and calls A0 until the estimated mass of working fluid in the loop has converged to the mass of working fluid actually filled in the loop. For the other conditions considered in Secs. II.C and II.D, the equations formulated there are used in Algorithm A2 with a modification to evaluate the thermodynamic state of the CC and the core [instead of only evaluating for the core (i.e., T_5 and ρ_5)]. Instead of just solving for only T_5 and ρ_5 as in the original Algorithm A2 for hard-filled condition, A2 is modified to solve the equation of state and the energy balance equation in the core, the CC, and the bayonet (simultaneously) for T_{4e}, ρ_{4e}, T_5, ρ_5, T_r, and ρ_r. The mass imbalance equation, as described in [3], is used to determine the thermodynamic state just above the meniscus (i.e., state point 0). Mass imbalance is the difference between the calculated mass in the loop, which is determined based on estimated temperature and density distribution in the loop and the specified mass of charge M_{tot}.

For the cases considered in this paper, the numerical scheme yields a temperature convergence better than 0.01 K, and the normalized global energy balance error is less than 1%. Mass imbalance in the hard-filled LHP is less than 0.05% of the total mass of working fluid M_{tot}.

Table 1 Brief summary of the functionality of various algorithms

Case	Solution algorithm
Saturated CC (Sec. II.A)	A1-LHP [3]. Solves Eq. (3) for T_5 in the core and the CC.[a]
Hard-fill assuming $T_r \sim T_5$ (Sec. II.B)	A2 [3]. Solves Eqs. (1) and (3) for T_5 and ρ_5 in the core and the CC.[a]
Without bayonet (Sec. II.C) and with bayonet (Sec. II.D)	A2 [3] is modified to solve for T_{4e}, ρ_{4e}, T_5, ρ_5, T_r, and ρ_r.[a]

[a]In addition to the other state points in the vapor line, the liquid line, and the condenser.

IV. Discussion of Loop Heat Pipe Operating Characteristics

A C-language program for steady-state simulation is developed on the basis of the methodology outlined previously. Steady-state system behavior of an LHP is studied with ammonia as the working fluid. Thermophysical properties of ammonia are obtained using REFPROP 7.0 FORTRAN source codes [11]. These FORTRAN source codes are integrated into the simulation program. In this paper, regime-based correlations proposed by Hajal et al. [15] and Thome et al. [16] are used for the evaluation of the condensation heat transfer coefficient and void fraction in the two-phase region of the condenser and the liquid line (if necessary). The details of the LHP used for the analysis are summarized in Table 2. The data presented in Table 2 are basically derived from the experimental setup discussed in [17]. The evaporation heat transfer coefficient H_{evap} used in this analysis (Table 2) is a conservative estimate for ammonia, based on the experimental observations presented in [18]. Unless explicitly stated, the operating characteristics discussed subsequently are based on the input data in Table 2. Steady-state behavior is simulated for various evaporator heat loads and masses of charge. The results of the simulation are discussed in this section. First, the operating characteristics of an LHP are presented on the basis of results for the case in which the core and the CC temperature are assumed to be nearly the same ($T_r \sim T_5$). This assumption holds for an LHP with a two-phase CC (non-hard-filled). Furthermore, it is shown that the operating characteristics of a hard-filled TAG LHP without a bayonet indicate that the assumption $T_r \sim T_5$ is valid. This is followed by an analysis of operating characteristics of a hard-filled TAG LHP with a bayonet. Table 3 lists the various cases that are analyzed in this section. Note that gravitational effects are not studied here. The term deprime is used extensively in subsequent sections and implies cessation of LHP operation.

Table 2 Summary of system parameters

Parameters	Values	Parameters	Values
Evaporator Wick[a]		*Condenser*	
L_w	200 mm	L_{cond}	3000 mm
D_{wo}	24.15 mm	$D_{\mathrm{cond},o}$	6.35 mm
D_{wi}	11 mm	$D_{\mathrm{cond},i}$	4.57 mm
H_{evap}	5000 W · m^{-2}·K^{-1}	$H_{\mathrm{cond},o}$	300 W · m^{-2}·K^{-1}
$H_{\mathrm{evap}-\infty}$	0 W · m^{-2}·K^{-1}	$k_{\mathrm{cond},t}$	15 W · m^{-1} · K^{-1}
D_p	10 μm		*CC*
k_w	1 W · m^{-1} K^{-1}	V_r	150 cm^3
K	10^{-13} m^2	$A_{r,o}$	0.017 m^2
Vapor and liquid lines		T_r	298.15 K
L_{vl}	1500 mm	L_{rt}	30 mm
L_{ll}	2000 mm	L_{b1}	20 mm
$D_{\mathrm{vl},o}$, $D_{\mathrm{ll},o}$	6.35 mm	k_{rt}	15 W · m^{-1}·K^{-1}
$D_{\mathrm{vl},i}$, $D_{\mathrm{ll},i}$	4.57 mm	H_{bo}	50 W·m^{-2}·K^{-1}
$k_{\mathrm{vl},t}$, $k_{\mathrm{ll},t}$	15 W · m^{-1}·K^{-1}	$U_{r-\infty}$	10 W · m^{-2}·K^{-1}
$H_{\mathrm{vl}-\infty}$, $H_{\mathrm{ll}-\infty}$	10 W · m^{-2}·K^{-1}		*Sink*
Ambient		T_{sink}	273.15 K
T_∞	298.15 K		

[a]Evaporator is assumed to have negligible heat transfer with surroundings.

Table 3 Summary of characteristic heat loads in LHP for different masses of charge in the system

	LHP			
M_{tot}	Q_{open}	Q_{hf}	Remarks	Results
135 g	450 W	1150 W	[a]	Fig. 6; Sec. IV.A
145 g	450 W	650 W	[a]	Figs. 3–8; Secs. IV.A–IV.C.
160 g	——	220 W	[b]	Figs. 5, 6, 9, and 10; Secs. IV.A and IV.C
165 g	——	180 W	[b]	Fig. 6; Sec. IV.A

[a]LHP hard fills after LHP opens.
[b]LHP hard fills before LHP opens. The condenser never opens in this case.

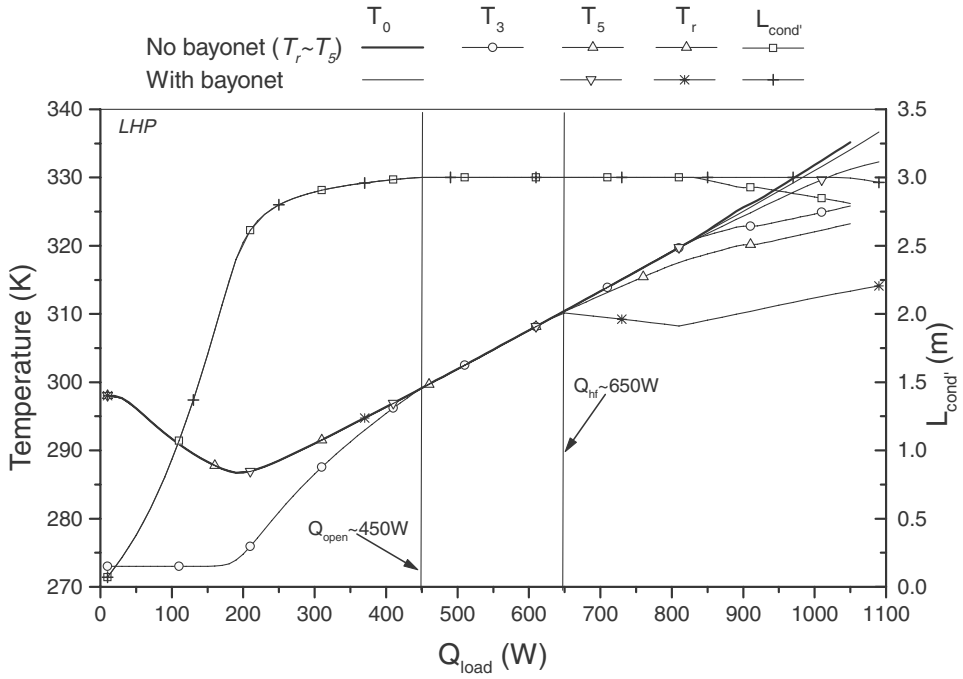

Fig. 3 Variation of T_0, T_3, T_5, and $L_{cond'}$ with Q_{load} in an LHP for $M_{tot} = 145$ g.

A. Case when $T_r = T_5$ is Applicable

Figure 3 shows the LHP operating temperature T_0 variation with heat load. The operating temperature curve has the classical $\surd$ shape (if the ambient temperature is higher than the sink temperature). The operating temperature is the saturation temperature just above the meniscus. It can also be approximated by the saturation temperature corresponding to the absolute pressure in the CC, because the pressure drop (from state points 1 to 5) in the LHP is not very large and $\frac{dP}{dT}|_{sat}$ is large for ammonia. The operating temperature reduces with an increase in heat load (for small heat loads), and the temperature of the liquid leaving the condenser T_3 is nearly constant (Fig. 3). The liquid in the liquid line picks up (or loses) heat depending on the ambient conditions. In this study, the ambient temperature is greater than the sink temperature. After a certain heat load, the condenser exit temperature increases because of the reduced subcooling length in the condenser. The load corresponding to maximum subcooling has a minimum operating temperature. Further increase in heat load results in higher operating temperature [3].

After a certain heat load Q_{open}, the entire length of the condenser is used for condensation, and the operating temperature increases linearly with heat load (Fig. 3). This happens because the length of the condenser available for heat rejection remains constant for heat loads beyond Q_{open}. Figure 4 shows that the quality of fluid at the condenser exit x_3 is greater than zero for heat loads exceeding Q_{open}. This is when the LHP is said to have moved into a constant conductance mode [5]. It is also observed in Fig. 4 that for heat loads greater than Q_{open}, x_4 becomes greater than zero, implying that vapor enters the core. In spite of vapor entering the core, an LHP does not deprime [5,12]. The latent heat associated with vapor leaving the liquid line $\dot{m}x_4h_{fg4}$ is lost to the ambient in the CC. This implies that the CC temperature (or operating temperature) is more than the ambient. Thus, the LHP operating temperature at which the

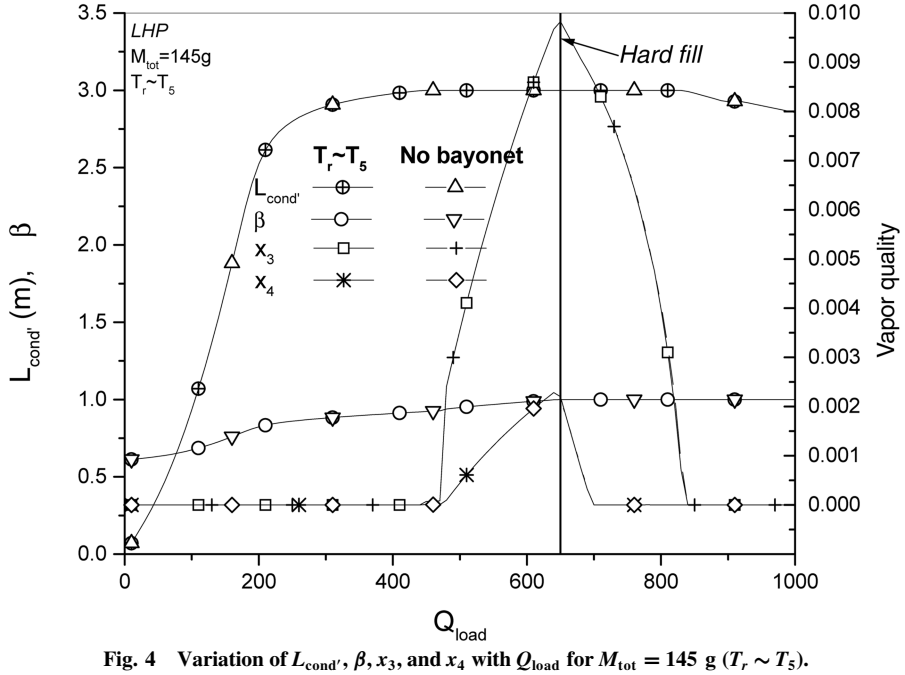

Fig. 4 Variation of $L_{cond'}$, β, x_3, and x_4 with Q_{load} for $M_{tot} = 145$ g ($T_r \sim T_5$).

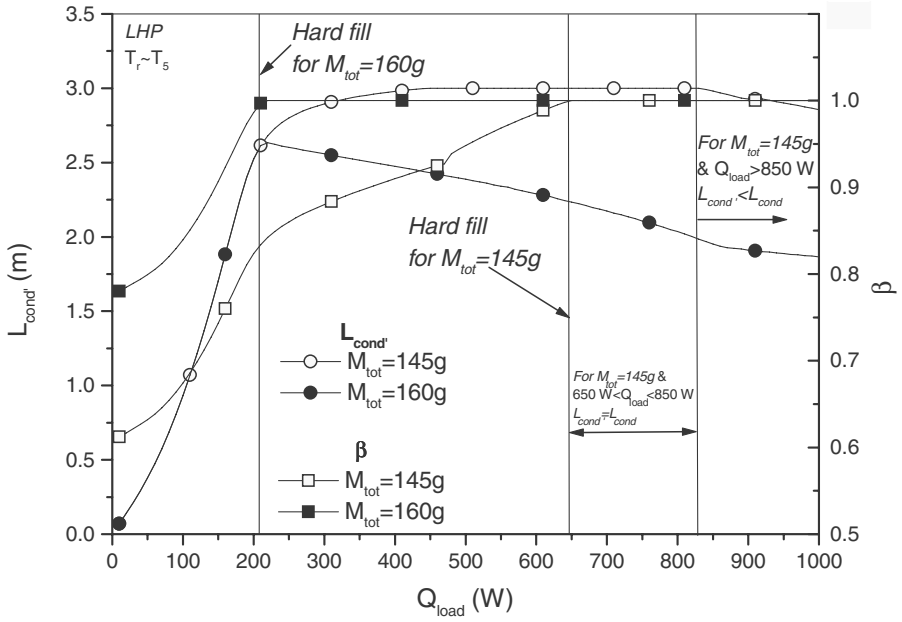

Fig. 5 Effect of a mass of charge on length of condensation and volume fraction of liquid in CC when $T_r \sim T_5$.

condenser opens is greater than or equal to the ambient. Hence, for heat loads greater than Q_{open}, the operating temperature is always more than the ambient.

Figure 5 illustrates the variation of the volume fraction of the liquid in the CC β with heat load in an LHP. Two masses of charge are considered: 145 and 160 g. The LHP characteristics are described first for 145 g, followed by a discussion on the effect of increasing the mass of charge. The heat loads at which the condenser opens and the LHP hard fills are given in Table 3. With the increase in heat load, more fluid is injected into the CC, resulting in an increase of β. This trend continues until the heat load reaches Q_{hf}, at which point the CC is full of liquid (hard-filled condition). Figure 5 shows that for $M_{\text{tot}} = 145$ g, β is unity (implying hard fill) for loads greater than 650 W. The core of a hard-filled LHP is subcooled, and the temperature difference across the wick increases, as seen in Fig. 3. When the LHP (with $M_{\text{tot}} = 145$ g) is hard-filled (Fig. 4), the condenser is already open and vapor enters the core. After the CC is hard-filled, the vapor quality at the condenser exit and at the liquid line exit reduces sharply. This is attributed to a steep rise in Q_{Lc} due to a larger temperature difference across the wick that increases the subcooling requirement [$\dot{m}C_{p,54}(T_5 - T_4)$, in Eq. (3)]. In the case $x_4 > 0$, the large temperature difference reduces the CC cooling capability of the fluid returning to the evaporator core [as given by $x_4\dot{m}h_{\text{fg}} + \dot{m}C_{p,54}(T_4 - T_5)$, from Eq. (3)]. A larger heat rejection requirement in the CC, the condenser, and the liquid line is realized by a steep rise in the operating temperature [3].

For heat loads greater than Q_{hf}, most of the vapor condenses in the liquid line due to the large temperature difference with the ambient, resulting from higher operating temperature. Figure 4 indicates that beyond 700 W, the vapor completely condenses in the liquid line, and no vapor enters the core/CC. Beyond 850 W, the vapor completely condenses in the condenser (i.e., $x_3 = 0$) and the condensation length starts reducing due to liquid expansion resulting from the higher operating temperature (see Fig. 5). Because the CC is full, any further increase in the operating temperature will cause the liquid to expand into the condenser. Once the liquid completely condenses in the condenser, subcooling increases at the condenser exit, and hence T_3 and T_0 diverge (Fig. 3). The operating temperature is higher than that

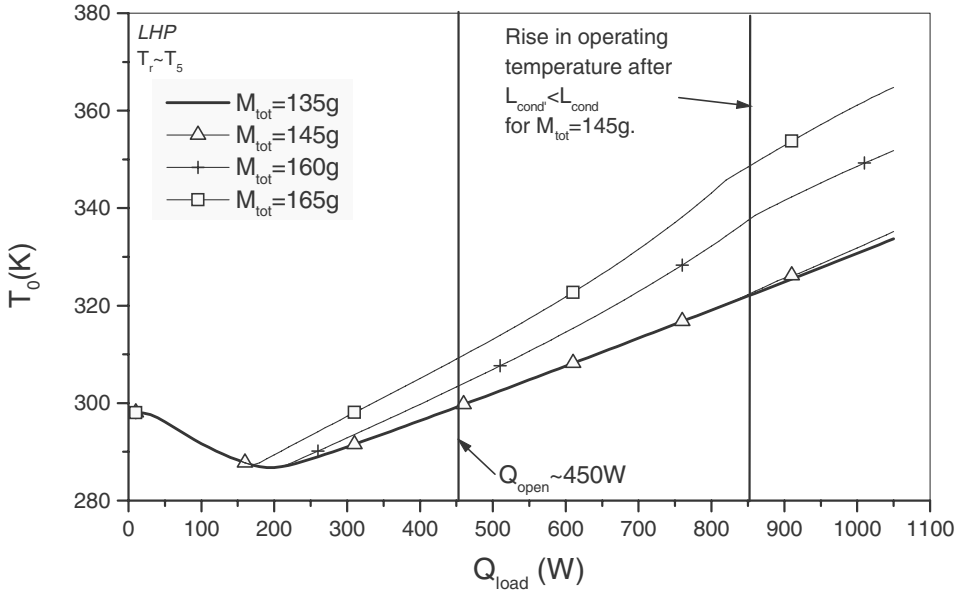

Fig. 6 Effect of mass of charge on LHP operating temperature when $T_r \sim T_5$.

in the non-hard-filled LHP only after condensation is limited to the condenser (Fig. 6). Although the temperature difference between the non-hard-filled ($M_{tot} = 135$ g) and the hard-filled LHP ($M_{tot} = 145$ g) appears to be nearly the same for the heat loads under consideration, this difference would continuously increase with heat load.

The mass of charge affects the load at which hard filling occurs Q_{hf}. Figure 5 shows that for the 145 g mass of charge, the CC hard fills after the condenser opens, whereas, for the 160 g mass of charge, the LHP hard-fills before the condenser can fully open. For a given system and boundary conditions, Q_{hf} reduces with an increase in mass of charge in the loop (Fig. 5). Figure 6 shows variation of operating temperature for different masses of charge in an LHP. As expected, with an increase in the mass of charge, the LHP hard fills at lower loads. In the system with a mass of charge of 135 g, the condenser fully opens at a heat load of 450 W and hard fills at about 1100 W. A system with 145 g of ammonia hard fills at about 650 W, although a perceptible rise in the operating temperature occurs only after the condensation length is less than the condenser length (i.e., when hard-filled). For a mass of charge of 160 g, the hard fill occurs at about 220 W, and a steep rise in operating temperature is observed thereafter. The CC of the LHP, with 160 g of ammonia, hard fills

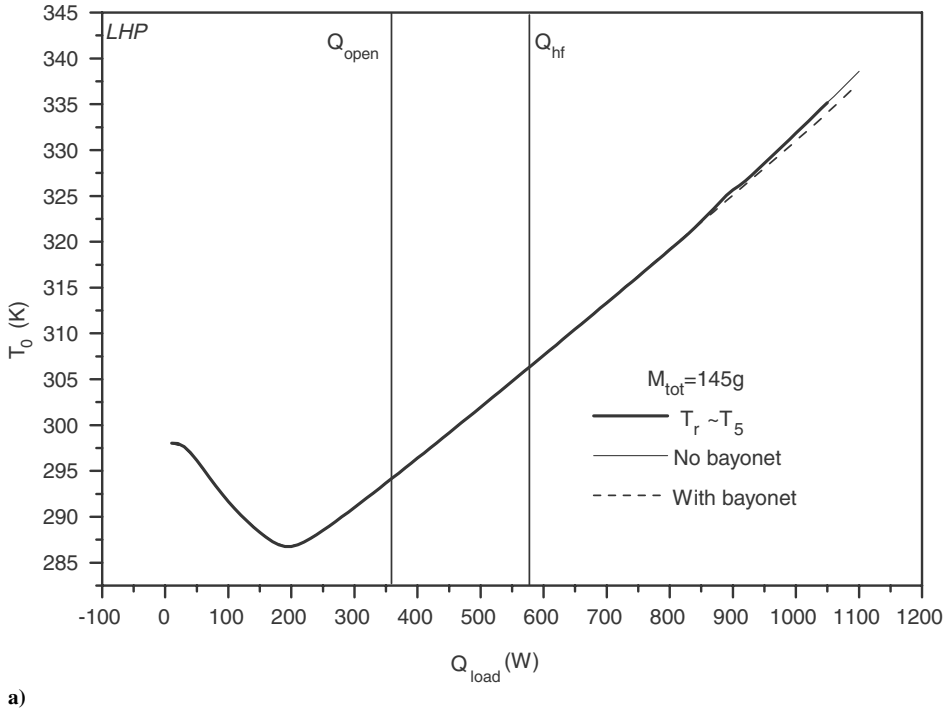

a)

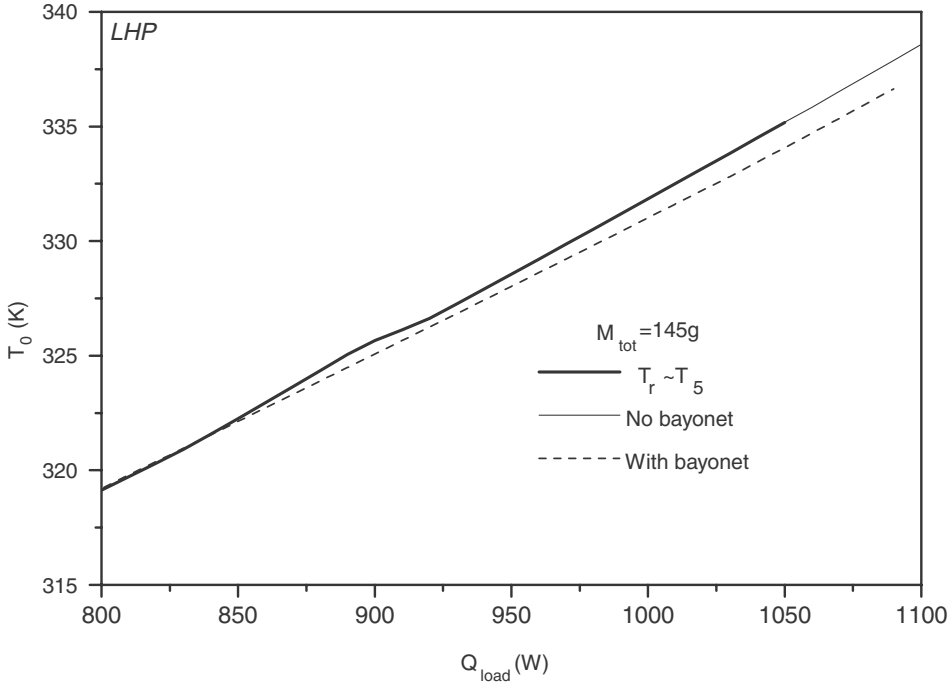

b)

Fig. 7 Effect of bayonet on LHP operating temperature with $M_{tot} = 145$ g. Hard fill occurs after condenser opens.

before the condenser fully opens. A steep rise in temperature is attributed to a decrease in length of condensation due to liquid expansion into the condenser. For an LHP with a 160 g charge, the operating temperature T_0 diverges from the non-hard-filled operating temperature curve, as seen in Fig. 6. For the 165 g case, the divergence of operating temperature, upon hard fill, occurs at lower loads. It may be noted that for this case, the operating temperature starts increasing even before the minimum operating temperature (287 K for this LHP with $M_t = 135$ g) is reached. This is similar to the case described by Maidanik [2], in which an increase in operating temperature with heat load (after initial drop in T_0) is attributed to hard filling of the CC. The behavior of LHP discussed previously is valid only in LHPs for which the assumption $T_r \sim T_5$ holds.

B. Tubular Axially Grooved Loop Heat Pipe Without a Bayonet and $T_r \neq T_5$

Figure 2a shows a schematic of a TAG LHP without a bayonet. It is seen in Fig. 7 that the LHP operating temperature without a bayonet (Sec. II.C) is nearly equal to that obtained with the assumption $T_r \sim T_5$ (Sec. II.B). Figure 4 shows that the variation of the condensation length, the vapor quality at the exit of the condenser, and the vapor quality at the liquid line exit are nearly identical when $T_r \sim T_5$ is assumed for an LHP without a bayonet. Thus, the assumption $T_r \sim T_5$ appears to be reasonable even for hard-filled LHPs without a bayonet.

C. Tubular Axially Grooved Loop Heat Pipe with a Bayonet and $T_r \neq T_5$

Figure 2b shows a schematic of a TAG LHP with a bayonet. For a mass of charge of 145 g, the LHP hard fills after the condenser opens. Figures 3 and 7 show that under hard-fill conditions, the operating temperature of a TAG LHP with a bayonet (as determined based on the analysis in Sec. II.D) is slightly different from that of an LHP without a bayonet. This difference will increase as the load on the evaporator is further increased. However, for the heat loads under consideration in Fig. 7, the temperatures in the two cases are not very different. Figure 7 also shows that the operating temperature in the constant conductance mode (without hard filling) is the same for all the cases considered. The LHP hard fill occurs at a heat load of 650 W ($M_{\text{tot}} = 145$ g). In the LHPs considered in this paper, the condenser opens at 450 W (provided the LHP does not hard fill below this load).

It is observed in Fig. 3 that the CC temperature in an LHP with a bayonet separates from the operating temperature immediately after hard fill. This does not occur in an LHP without a bayonet. Also, the core temperature continues to be nearly the same as the operating temperature until the heat load reaches 1050 W. The large difference in the core and the CC temperature (in an LHP with a bayonet) is attributed to weak thermal coupling between them. In an LHP without a bayonet, good convective thermal coupling is achieved by the subcooled liquid flowing from the CC into the core. In an LHP with a bayonet, the CC does not contribute to the cooling of the core and is hence at a significantly lower temperature than the operating temperature. The small mass flow of the cold liquid from the CC to the core $\dot{m}x_{4e}$ via the secondary wick helps compensate for the heat leak to the core Q_{Lc} and also contributes to the little subcooling that may occur. This results in a warmer core (compared with CC) and hence the temperature of the core can be very closely approximated by the operating temperature until the heat load is about 800 W.

Figure 8 shows that for LHPs in which hard filling occurs after the condenser has completely opened (i.e., $x_3 > 0$) and vapor enters the core, the presence of a bayonet influences the variation of vapor quality at the exit of the condenser x_3 and the liquid line x_4. The liquid line exit quality x_4 reduces immediately after hard filling, whereas x_3 continues to increase for some time beyond hard filling and then reduces after $x_4 = 0$, which corresponds to a heat load of 800 W. At this heat load, the core temperature curve separates from the operating temperature curve, as no vapor enters the core (see Fig. 3). The drop in x_4 with a bayonet is not as steep as that without it ($T_r \sim T_5$). This is attributed to higher x_3 in the case of the LHP with a bayonet. The vapor quality at the exit of the condenser x_3 reduces after 800 and up to 1050 W, beyond which the two-phase front (two-phase region) is restricted in the condenser only. For an LHP without a bayonet, the two-phase front is restricted to the condenser (i.e., $x_3 = 0$) at a heat load of 850 W. This explains the interesting observation that the operating temperature curve for an LHP without a bayonet separates from an LHP with a bayonet for heat loads beyond 850 W. The two-phase front in an LHP without a bayonet is restricted in the condenser, which is confirmed by the fact that $x_3 = 0$ and $L_{\text{cond}'} < L_{\text{cond}}$ for heat loads of more than 850 W (Fig. 8). Beyond

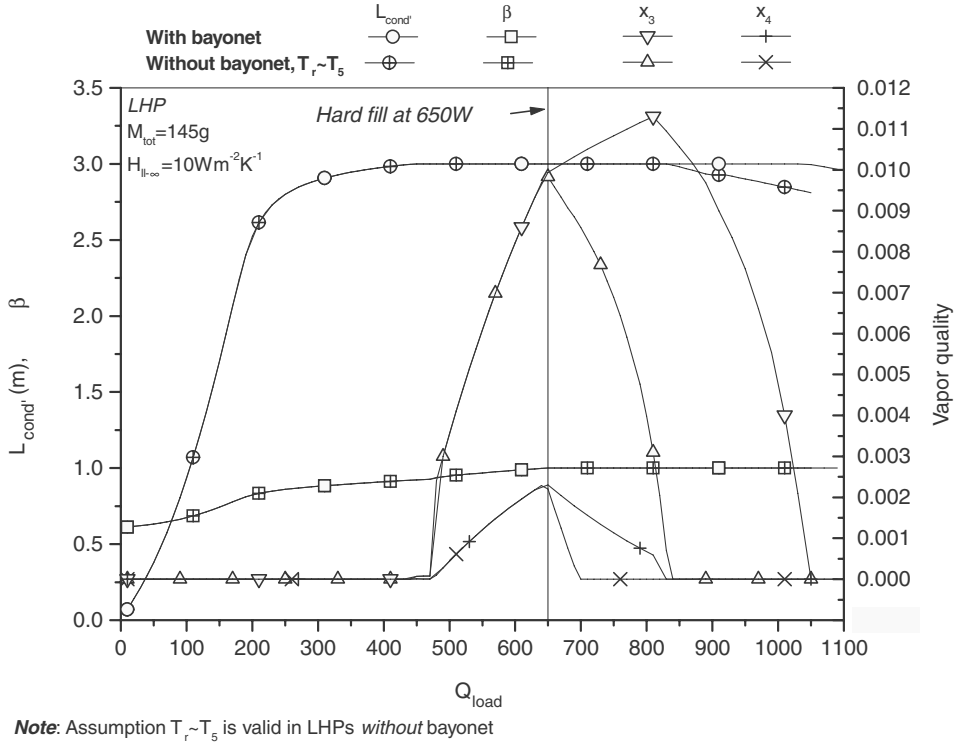

Note: Assumption $T_r \sim T_5$ is valid in LHPs *without* bayonet

Fig. 8 Effect of bayonet on $L_{\text{cond}'}$, β, x_3, and x_4 in an LHP with $M_{\text{tot}} = 145$ g and $H_{\text{ll}-\infty} = 10$ W · m^{-2}·K^{-1}.

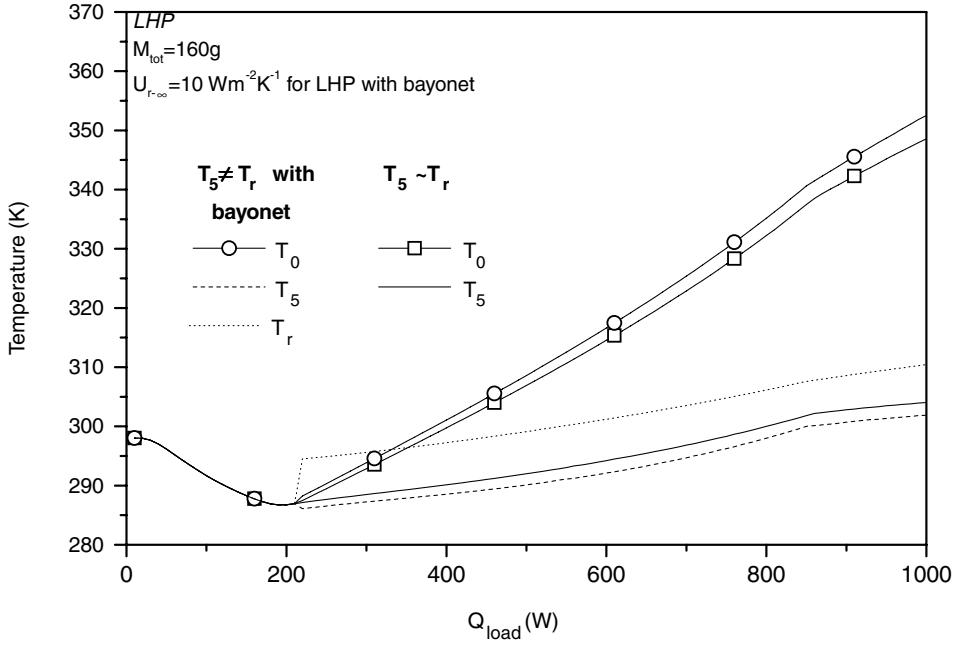

Fig. 9 Effect of bayonet on temperatures in an LHP with 160 g of ammonia.

1050 W, the temperature for an LHP with a bayonet rises steeply. This is attributed to the withdrawal of the two-phase front into the condenser, which is evident in Fig. 8 ($L_{\text{cond}'} < L_{\text{cond}}$ and $x_3 = 0$ for $Q_{\text{load}} > 1050$ W). The previously discussed operating characteristics are expected from an LHP that hard fills after the condenser opens.

A significant departure of the operating temperature in an LHP with a bayonet (compared with that without a bayonet) is seen in Fig. 9 for a higher mass of charge (160 g) in which hard fill occurs before the condenser completely opens. This departure increases with the mass of charge. When a bayonet is present and hard filling occurs before the condenser completely opens, the CC temperature suddenly rises (because the operating temperature is less than the ambient) and the liquid in the CC becomes superheated (i.e., $T_r > T_{\text{sat}}$). This is attributed to strong thermal coupling between the CC and the ambient $U_{r-\infty}$, compared with that between the CC fluid and the relatively colder core (and the bayonet). The system would probably cease to operate if the fluid in the CC flashes, which in turn depends on the degree of incipient superheat for boiling ($T_r - T_0 >$ incipient superheat). Thus, TAG-LHP systems (with a bayonet), for which the CC is not insulated, cannot operate when hard-filled if the hard fill occurs before the condenser opens and the ambient temperature is higher than the sink.

Figure 10 shows the operating characteristics of the TAG LHP with a bayonet and with a well-insulated CC. It is noticed that the rise in the CC temperature is small (because of weak thermal coupling with the warmer ambient), thus if the liquid in the CC can withstand the superheat without flashing, the LHP will continue to operate. At higher heat loads, the CC temperature is lower than the saturation temperature and thus will not deprime. The CC temperature in LHPs, with the CC isolated from the ambient, is chiefly dictated by the heat leakage from the evaporator. Such an LHP will continue to operate if Q_{Lr} is matched by cooling, due to the (subcooled) liquid flowing through the bayonet as it traverses the CC. Note that the liquid entering the CC is subcooled [i.e., $T_4 < T_{\text{sat}}(P_r)$] because the liquid leaving the condenser is subcooled.

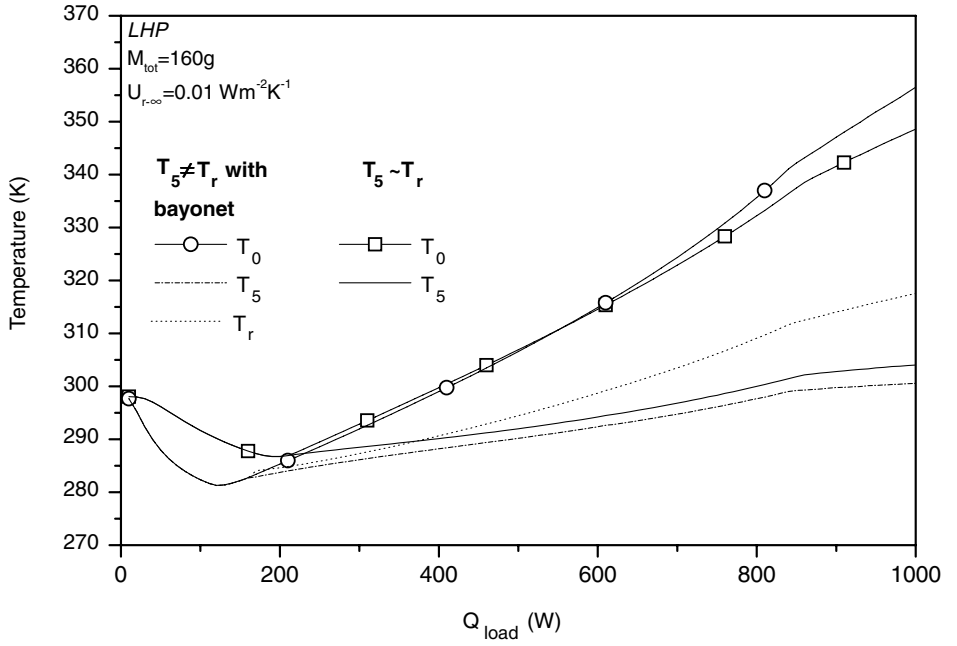

Fig. 10 Effect of bayonet on temperatures in an LHP with the CC insulated [$U_{r-\infty} = 0.01$ W·m^{-2} · K^{-1}] and 160 g of ammonia.

It is well known that liquid inventory and its distribution are very important in the operation of LHPs, based on the studies by Ku [5] and Pastukhov et al. [4]. Pastukhov et al. proposed that a bayonet and a secondary wick together can ensure successful startup under microgravity conditions. Large liquid inventory in LHPs also helps ensure that the primary wick is always wetted. Based on the preceding case studies, it is inferred that LHPs that hard fill after the condenser opens do not deprime (i.e., continue to operate).

V. Conclusions

A theoretical study based on a mathematical model was undertaken to study the issues underlying hard fill in LHPs with and without a bayonet. The cases analyzed in this paper assumed that the ambient temperature was greater than the sink temperature. The results of this study indicate that the mass of charge and the presence of a bayonet have significant influence on LHP operation. With larger masses of charge, the heat load at which hard filling occurs reduces. Further, the LHP operating temperature shows a steep rise after hard filling.

In LHPs with an FP evaporator and those with a TAG evaporator without a bayonet, the hard fill does not pose a risk of deprime. The CC fluid temperature and the core temperature are nearly equal in such hard-filled LHPs, and their operating characteristics are significantly different from hard-filled TAG LHPs with a bayonet. The core temperature and the CC temperature in such an LHP (with a bayonet) are different. The results of this theoretical study of a TAG LHP (with a bayonet) for which the CC is not insulated suggest that

1) If hard fill occurs after the condenser opens, the operating temperature shows a steep rise after the two-phase front is limited to the condenser. In this case, the LHP is not susceptible to deprime after hard fill.

2) If hard fill occurs before the condenser opens, the CC fluid gets significantly superheated upon hard fill (due to good coupling with the surrounding) and the CC fluid is likely to flash. Hard-filled LHPs in this case are susceptible to deprime.

If the CC is the insulated for a TAG LHP (with a bayonet)

1) Hard fill occurs before the condenser completely opens and the CC temperature is not significantly superheated due to weak thermal coupling between the CC and the ambient.

2) Deprime is dictated by how much CC superheat (due to heat leak from the evaporator) the system can withstand.

An interesting observation for LHPs (whether the CC is insulated or not) for which hard fill occurs after the condenser opens is that the operating temperature at which the condenser opens must be equal to or greater than the ambient temperature.

Acknowledgments

This work was carried out at Indian Space Research Organisation (ISRO) Satellite Centre. The authors are grateful to D. R. Bhandari, K. Badari Narayana, S. C. Rastogi, S. G. Barve and D. Chakraborty from ISRO Satellite Centre for encouragement and support.

References

[1] Ku, J., "Recent Advances in Capillary Pumped Loop Technology," AIAA 1997 National Heat Transfer Conference, AIAA Paper 97-3780, 1997.

[2] Maidanik, Y. F., "Loop Heat Pipes," *Applied Thermal Engineering*, Vol. 25, Apr. 2005, pp. 635–657. doi:10.1016/j.applthermaleng.2004.07.010

[3] Adoni, A. A., Ambirajan, A., Jasvanth, V. S., Kumar, D., Dutta, P., and Srinivasan, K., "Thermohydraulic Modeling of Capillary Pumped Loop and Loop Heat Pipe," *Journal of Thermophysics and Heat Transfer*, Vol. 21, No. 2, 2007, pp. 410–421. doi:10.2514/1.26222

[4] Pastukhov, V. G., Maidanik, Y. F., and Fershtater, Y. G., "Adaptation of Loop Heat Pipes to Zero-G Conditions," *Proceedings of the Sixth European Symposium on Space Environmental Control Systems*, No. SP-400, ESA, Noordwijk, The Netherlands, 1997, pp. 385–391.

[5] Ku, J., "Operating Characteristics of Loop Heat Pipes," Society of Automotive Engineers Paper 1999-01-2007, 1999.

[6] Kaya, T., and Hoang, T. T., "Mathematical Modelling of Loop Heat Pipes and Experimental Validation," *Journal of Thermophysics and Heat Transfer*, Vol. 13, No. 3, 1999, pp. 314–320. doi:10.2514/2.6461

[7] Chuang, P.-Y. A., "An Improved Steady-State Model of Loop Heat Pipes Based on Experimental and Theoretical Analysis," Ph.D. Thesis, Pennsylvania State Univ., University Park, PA, 2003.

[8] Launay, S., Sartre, V., and Bonjour, J., "Analytical Model for Characterization of Loop Heat Pipes," *Journal of Thermophysics and Heat Transfer*, Vol. 22, No. 4, 2008, pp. 623–631. doi:10.2514/1.37439

[9] Guiping, L., Hongxing, Z., Xingguo, S., Jianfeng, C., Ting, D., and Jianyin, M., "Development and Test Results of a Dual Compensation Chamber Loop Heat Pipe," *Journal of Thermophysics and Heat Transfer*, Vol. 20, No. 4, 2006, pp. 825–834. doi:10.2514/1.21858

[10] Adoni, A. A., Ambirajan, A., and Jasvanth, V. S., "Aspects of Thermohydraulic Modelling of Capillary Pumped Loop and Loop Heat Pipe," Indian Space Research Organisation Satellite Centre, TR ISRO-ISAC-TR-0809, Bangalore, India, June 2007.

[11] Lemmon, E. W., McLinden, M. O., and Huber, M. L., *User Guide: NIST Reference Fluid Thermodynamic and Transport Properties, RE-FPROP: Version 7.0*, National Inst. of Standards and Technology, Boulder, CO, Aug. 2002.

[12] Parker, M. L., "Modeling of Loop Heat Pipes with Applications to Spacecraft Thermal Control," Ph.D. Thesis, Univ. of Pennsylvania, Philadelphia, 2000.

[13] Rohsenow, W. M., Hartnett, J. P., and Cho, Y. I. (eds.), *Handbook of Heat Transfer*, McGraw–Hill, New York, 1998.

[14] Chapra, S. C., and Canale, R. P., *Numerical Methods for Engineers*, McGraw–Hill, New York, 2002.

[15] Hajal, J. E., Thome, J. R., and Cavallini, A., "Condensation in Horizontal Tubes, Part 1: Two-Phase Flow Pattern Map," *International Journal of Heat and Mass Transfer*, Vol. 46, No. 18, 2003, pp. 3349–3363. doi:10.1016/S0017-9310(03)00139-X

[16] Thome, J. R., Hajal, J. E., and Cavallini, A., "Condensation in Horizontal Tubes, Part 2: New Heat Transfer Model Based on Flow Regimes," *International Journal of Heat and Mass Transfer*, Vol. 46, No. 18, 2003, pp. 3365–3387. doi:10.1016/S0017-9310(03)00140-6

[17] Adoni, A. A., Ambirajan, A., Jasvanth, V. S., Kumar, D., and Dutta, P., "Effects of Mass of Charge on Loop Heat Pipe Operational Characteristics," *Journal of Thermophysics and Heat Transfer*, Vol. 23, No. 2, 2009, pp. 346–355. doi:10.2514/1.41618

[18] Jasvanth, V. S., Adoni, A. A., Ambirajan, A., and Kumar, D., "Results of Experimental and Theoretical Study of Ammonia Based Loop Heat Pipe," *Journal of Spacecraft Technology*, Vol. 19, Jan. 2009, pp. 18–31.